Physica E 43 (2011) 651–656

Contents lists available at ScienceDirect

Physica E

journal homepage: www.elsevier.com/locate/physe

Theory of the electronic and transport properties of graphene under a periodic electric or magnetic field

Cheol-Hwan Park [a,b], Liang Zheng Tan [a,b], Steven G. Louie [a,b,*]

[a] Department of Physics, University of California at Berkeley, Berkeley, California 94720, United States
[b] Materials Sciences Division, Lawrence Berkeley National Laboratory, Berkeley, California 94720, United States

ARTICLE INFO

Available online 3 August 2010

ABSTRACT

We discuss the novel electronic properties of graphene under an external periodic scalar or vector potential, and the analytical and numerical methods used to investigate them. When graphene is subjected to a one-dimensional periodic scalar potential, owing to the linear dispersion and the chiral (pseudospin) nature of the electronic states, the group velocity of its carriers is renormalized highly anisotropically in such a manner that the velocity is invariant along the periodic direction but is reduced the most along the perpendicular direction. Under a periodic scalar potential, new massless Dirac fermions are generated at the supercell Brillouin zone boundaries. Also, we show that if the strength of the applied scalar potential is sufficiently strong, new zero-energy modes may be generated. With the periodic scalar potential satisfying some special conditions, the energy dispersion near the Dirac point becomes quasi one-dimensional. On the other hand, for graphene under a one-dimensional periodic vector potential (resulting in a periodic magnetic field perpendicular to the graphene plane), the group velocity is reduced isotropically and monotonically with the strength of the potential.

1. Introduction

Graphene is a single atomic layer of carbon atoms arranged in a honeycomb structure. The electronic states in graphene obey a unique linear energy dispersion relation near the Fermi energy (Fig. 1(a)), and they possess an additional quantum number called pseudospin which describes the electron's probability amplitudes at the two different sublattices of carbon atoms forming graphene [1]. These behaviors are similar to those of massless neutrinos in relativistic quantum physics except that the role played by the actual spin of the neutrinos is now replaced by the pseudospin in graphene.

When graphene is subjected to a slowly varying nanoscale external periodic scalar or vector potential, the quasiparticles in graphene show even more interesting physics. Recently, there have been several studies on the electronic properties of graphene under either a periodic scalar potential [2–11], under a periodic vector potential [12–18], or under a periodic corrugation [19–21].

Graphene superlattices are not just theorists' dream but have been experimentally realized. Superlattice patterns with periodicity as small as 5 nm have been imprinted on graphene through electron-beam induced deposition of adsorbates [22], triangular patterns with $\sim$10 nm lattice period have been observed for graphene on metal surfaces [23–29], and periodically corrugated graphene sheet has also been reported [30]. Periodically patterned gates can provide another route for making graphene superlattices.

In this paper, we review the electronic properties of charge carriers in graphene under an external periodic scalar or vector potential. Especially, we focus on one-dimensional (1D) periodic potentials (e.g., Fig. 1(b) or (c)) for simplicity. However, many of the essential findings discussed here are applicable to two-dimensional (2D) periodic potentials. We also discuss the methodologies used in the analytical and numerical calculations.

The rest of the paper is organized as follows. In Sections 2 and 3, we present the analytical derivation of the energy–momentum dispersion relation near the Dirac points (original or newly generated) in graphene under an external periodic scalar potential and vector potential, respectively. In Section 4, we present the details of our numerical calculations used in studying the effects of stronger perturbing potentials. In Section 5, we discuss the emerging massless Dirac fermions and quasi-1D modes under a strong external periodic scalar potential. Finally, in Section 6, we summarize our findings.

2. Graphene under an external periodic scalar potential

In this section, through analytical calculations, we show that when a 1D periodic scalar potential is applied to graphene: (i) the group velocity of the massless Dirac fermions is anisotropically

* Corresponding author at: Department of Physics, University of California at Berkeley, Berkeley, California 94720, United States.
E-mail address: sglouie@berkeley.edu (S.G. Louie).

1386-9477/$ - see front matter © 2010 Elsevier B.V. All rights reserved.
doi:10.1016/j.physe.2010.07.022

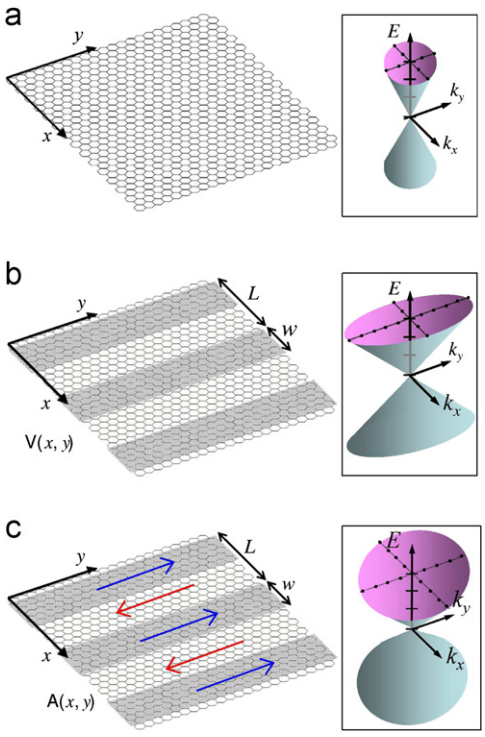

Fig. 1. (a) Schematic diagram of graphene. Inset: the linear and isotropic energy dispersion near one of the Dirac points in graphene. (b) A 1D graphene superlattice formed by Kronig–Penney type of scalar potential $V(x,y)=V(x)$ periodic along the x direction with spatial period L. The potential is $U_0/2$ in the grey regions and $-U_0/2$ outside. Inset: energy dispersion of charge carriers in this graphene superlattice. The energy dispersion along any line in 2D wavevector space going through the Dirac point is linear but with different group velocity. For a particle moving parallel to the periodic direction, the group velocity is not renormalized at all whereas that for a particle moving perpendicular to the direction of periodicity is reduced the most. (c) A 1D graphene superlattice formed by Kronig–Penney type of vector potential $\mathbf{A}(x,y)=A_y(x)\hat{y}$ periodic along the x direction with spatial period L. The vector potential $A_y(x)$ is $A_0/2$ in the grey regions and $-A_0/2$ outside. Inset: energy dispersion of charge carriers in this graphene superlattice. The group velocity around the Dirac point is reduced *isotropically*.

renormalized in momentum space in an unexpected fashion, and (ii) new massless Dirac fermions are generated at the supercell Brillouin zone boundaries [6].

We consider a situation where the spatial variation of the external periodic potential is much slower than the inter-carbon distance so that inter-valley scattering between the **K** and **K′** points in the Brillouin zone may be neglected [31,32]. We shall further limit our discussion to the low-energy electronic states of graphene which have wavevector **k**+**K** close to the **K** point, i.e. with $|\mathbf{k}| \ll |\mathbf{K}|$.

There are two carbon atoms per unit cell in graphene, forming two different sublattices. Hence the eigenstate of charge carriers in graphene can be represented by a two component basis vector. The Hamiltonian of the low-energy quasiparticles in pristine graphene in a pseudospin basis, $\begin{pmatrix}1\\0\end{pmatrix}e^{i\mathbf{k}\cdot\mathbf{r}}$ and $\begin{pmatrix}0\\1\end{pmatrix}e^{i\mathbf{k}\cdot\mathbf{r}}$, where $\begin{pmatrix}1\\0\end{pmatrix}$ and $\begin{pmatrix}0\\1\end{pmatrix}$ symbolically represent Bloch sums of $\pi-$orbitals with wavevector **K** on the sublattices A and B, respectively, is given by [33]

$$H_0 = \hbar v_0(-i\sigma_x\partial_x - i\sigma_y\partial_y), \tag{1}$$

where v_0 is the band velocity and the σ's are the Pauli matrices. The eigenstates and the energy eigenvalues are given by

$$\psi^0_{s,\mathbf{k}}(\mathbf{r}) = \frac{1}{\sqrt{2}}\begin{pmatrix}1\\ se^{i\theta_\mathbf{k}}\end{pmatrix}e^{i\mathbf{k}\cdot\mathbf{r}} \tag{2}$$

and

$$E^0_s(\mathbf{k}) = s\hbar v_0 k, \tag{3}$$

respectively, where $s=\pm 1$ is the band index and $\theta_\mathbf{k}$ is the angle between **k** and the $+k_x$ direction.

We now assume that a 1D scalar potential $V(x)$, periodic along the x direction with periodicity L, is applied to graphene (Fig. 1(b)). The Hamiltonian H then reads

$$H = \hbar v_0(-i\sigma_x\partial_x - i\sigma_y\partial_y + IV(x)/\hbar v_0), \tag{4}$$

where I is the 2×2 identity matrix. Next we perform a similarity transform, $H' = U_1^\dagger H U_1$, using the unitary matrix

$$U_1 = \frac{1}{\sqrt{2}}\begin{pmatrix} e^{-i\alpha(x)/2} & -e^{i\alpha(x)/2} \\ e^{-i\alpha(x)/2} & e^{i\alpha(x)/2}\end{pmatrix}, \tag{5}$$

where $\alpha(x)$ is given by

$$\alpha(x) = 2\int_0^x V(x')\,dx'/\hbar v_0. \tag{6}$$

Here, without losing generality, we shall assume that an appropriate constant has been subtracted from $V(x)$ and that $V(x)$ has been shifted along the x direction so that the averages of both $V(x)$ and $\alpha(x)$ are zero. The transformed Hamiltonian H' takes the form

$$H' = \hbar v_0\begin{pmatrix} -i\partial_x & -e^{i\alpha(x)}\partial_y \\ e^{-i\alpha(x)}\partial_y & i\partial_x\end{pmatrix}. \tag{7}$$

A similar transform has been used to study nanotubes under a sinusoidal potential [34,35].

We are interested in the low-energy quasiparticle states whose wavevector $\mathbf{k}\equiv\mathbf{p}+\mathbf{G}_m/2$ (where $\mathbf{G}_m = m(2\pi/L)\hat{x}\equiv mG\hat{x}$ is a reciprocal vector) is such that $|\mathbf{p}|\ll G$. In this case, we could treat the terms containing ∂_y in Eq. (7) as a perturbation. Also, to a good approximation, H' may be reduced to a 2×2 matrix using the following two states as basis functions

$$\begin{pmatrix}1\\0\end{pmatrix}' e^{i(\mathbf{p}+\mathbf{G}_m/2)\cdot\mathbf{r}} \quad\text{and}\quad \begin{pmatrix}0\\1\end{pmatrix}' e^{i(\mathbf{p}-\mathbf{G}_m/2)\cdot\mathbf{r}}. \tag{8}$$

Here, we should note that the spinors $\begin{pmatrix}1\\0\end{pmatrix}'$ and $\begin{pmatrix}0\\1\end{pmatrix}'$ now have a different meaning from $\begin{pmatrix}1\\0\end{pmatrix}$ and $\begin{pmatrix}0\\1\end{pmatrix}$.

In order to calculate these matrix elements, we perform a Fourier transform of $e^{i\alpha(x)}$

$$e^{i\alpha(x)} = \sum_{l=-\infty}^{\infty} f_l[V]e^{ilGx}, \tag{9}$$

where the Fourier components $f_l[V]$'s are determined by the periodic potential $V(x)$. We should note that in general

$$|f_l| < 1, \tag{10}$$

which can directly be deduced from Eq. (9). The physics simplifies when the external potential $V(x)$ is an even function and hence $\alpha(x)$ in Eq. (6) is an odd function. If we take the complex conjugate of Eq. (9) and change x to $-x$, it is evident that $f_l[V]$'s are real. General cases other than even potentials are discussed in Ref. [6]. For states with wavevector **k** very close to $\mathbf{G}_m/2$, the 2×2 matrix M whose elements are calculated from the Hamiltonian H' with the basis given by Eq. (8) can be written as

$$M = \hbar v_0(p_x\sigma_z + f_m p_y\sigma_y) + \hbar v_0 mG/2I. \tag{11}$$

After performing yet another similarity transform $M' = U_2^\dagger M U_2$ with

$$U_2 = \frac{1}{\sqrt{2}}\begin{pmatrix}1 & 1\\ -1 & 1\end{pmatrix}, \tag{12}$$

we obtain the final result:

$$M' = \hbar v_0(p_x\sigma_x + f_m p_y\sigma_y) + \hbar v_0 mG/2I. \quad (13)$$

The energy eigenvalue of the matrix M' is given by

$$E_s(\mathbf{p}) = s\hbar v_0\sqrt{p_x^2 + |f_m|^2 p_y^2} + \hbar v_0 mG/2. \quad (14)$$

Eq. (14) holds in general and not only for cases where the potential $V(x)$ is even [6]. The only difference of the energy spectrum in Eq. (3) from that in Eq. (14), other than a constant energy term, is that the group velocity of quasiparticles moving along the y direction has been changed from v_0 to $|f_m|v_0$. Thus, the electronic states near $\mathbf{k}=\mathbf{G}_m/2$ are also those of massless Dirac fermions but having a group velocity varying *anisotropically* depending on the propagation direction. The group velocity along the x direction is unchanged independent of the potential. Moreover, the group velocity along the y direction is *always lower* than v_0 (Eq. (10)) regardless of the form or magnitude of the periodic potential $V(x)$ as schematically depicted in Fig. 1(b).

We have thus shown that other than the original Dirac points, new massless Dirac fermions are generated around the supercell Brillouin zone boundaries, i.e., the case with non-zero m values in Eq. (14). It has also been shown that these newly generated massless Dirac points are the only available states in a certain energy window if graphene is subjected to a 2D repulsive periodic scalar potential having triangular symmetry [6].

One more thing to note is that in graphene under an external periodic scalar potential, a generalized pseudospin vector can be defined and used to describe the scattering properties between eigenstates; and especially, back-scattering processes by a slowly varying impurity potential are suppressed as in pristine graphene [6].

3. Graphene under a 1D external periodic vector potential

Now we move on to the case where a 1D vector potential $\mathbf{A}(x,y) = A_y(x)\hat{y}$ is applied to graphene (Fig. 1(c)). We show through a novel transformation relation between scalar and vector potentials [18] that, unlike the electrostatic case, the group velocity of charge carriers in graphene under a 1D periodic vector potential is renormalized *isotropically*.

The superlattice Hamiltonian, following the Peierls substitution, is given by

$$H = \hbar v_0(-i\sigma_x\partial_x - i\sigma_y\partial_y - \sigma_y eA_y(x)/\hbar c), \quad (15)$$

where e is the charge of an electron ($e<0$) and c is the speed of light. The time-dependent Dirac equation then reads

$$i\hbar\frac{d\psi}{dt} = \hbar v_0(-i\sigma_x\partial_x - i\sigma_y\partial_y - \sigma_y eA_y(x)/\hbar c)\psi. \quad (16)$$

Writing the wavefunction as $\psi(x,y;t) = e^{-iEt/\hbar}e^{ik_y y}\varphi(x)$, the Dirac equation becomes

$$E\varphi(x) = \hbar v_0(-i\sigma_x\partial_x + \sigma_y k_y - \sigma_y eA_y(x)/\hbar c)\varphi(x). \quad (17)$$

Now, if we multiply Eq. (17) by σ_y on both sides, define $\varphi'(x) = U_3\varphi(x)$ with

$$U_3 = \frac{1}{\sqrt{2}}\begin{pmatrix} 1 & 1 \\ 1 & -1 \end{pmatrix}, \quad (18)$$

and use the relations $U_3 = U_3^\dagger = U_3^{-1}$, $U_3\sigma_y U_3 = -\sigma_y$, and $U_3\sigma_x U_3 = \sigma_z$, Eq. (17) becomes

$$E'\varphi'(x) = \hbar v_0(-i\sigma_x\partial_x + \sigma_y k'_y + IV'(x)/\hbar v_0)\varphi'(x). \quad (19)$$

Here, we have defined

$$E' = -i\hbar v_0 k_y, \quad (20)$$

$$k_{y'} = iE/\hbar v_0, \quad (21)$$

and

$$V'(x) = -ie(v_0/c)A_y(x). \quad (22)$$

Eq. (19) is thus equivalent to the Dirac equation with a periodic scalar potential in Eq. (4) except that now the variables are imaginary numbers. Using analytic continuation [18], we obtain the energy–momentum dispersion relation in magnetic graphene superlattices from that in electrostatic graphene superlattices. For the states near the original Dirac point, as shown in the previous section, the energy dispersion in graphene under a periodic scalar potential is given (from Eq. (14)) by

$$E_s(\mathbf{k}) = s\hbar v_0\sqrt{k_x^2 + |f_0|^2 k_y^2}, \quad (23)$$

where according to Eq. (9)

$$f_0 = \frac{1}{L}\int_0^L \exp\left(i\int_0^x \frac{2}{\hbar v_0}V(x')\,dx'\right)dx. \quad (24)$$

Plugging Eqs. (20)–(22) into Eq. (23), we obtain

$$E_s(\mathbf{k}) = s\frac{1}{|f'_0|}\hbar v_0\sqrt{k_x^2 + k_y^2}, \quad (25)$$

where

$$f'_0 = \frac{1}{L}\int_0^L \exp\left(\int_0^x \frac{2e}{\hbar c}A_y(x')\,dx'\right)dx. \quad (26)$$

Therefore, from Eq. (25), we find that the group velocity in graphene under an external periodic vector potential (corresponding to a perpendicular magnetic field) is renormalized *isotropically* in the k_x–k_y space [17,18] even though the external vector potential profile is highly anisotropic in the x–y plane (Fig. 1(c)). Note from Eq. (26) that

$$|f'_0| > 1 \quad (27)$$

regardless of the form of the vector potential $A_y(x)$, i.e., the group velocity in graphene under an external periodic vector potential is always reduced. This result can in fact be used as a special case to understand the predictions of velocity reduction in metallic carbon nanotubes and gap reduction in semiconducting carbon nanotubes under a magnetic field [36,37].

4. Numerical calculation

If one wants to find the energy eigenvalues and eigenfunctions of graphene under an external periodic potential with wavevector $\mathbf{k}$ not very close to the supercell Brillouin zone boundary centers ($\mathbf{G}_m/2$), one has to resort to numerical calculations. Such numerical calculations have led us to the discovery of solutions corresponding to new branches of massless Dirac fermions [8] that are not found in the analytical calculations discussed in the previous sections.

The scattering amplitudes arising from the periodic scalar and vector potentials between eigenstates of pristine graphene (Eq. (2)), using the Hamiltonians in Eq. (4) and in Eq. (15), are given by

$$\langle\psi^0_{s,\mathbf{k}}|IV(\mathbf{r})|\psi^0_{s',\mathbf{k}'}\rangle = \sum_{\mathbf{G}}\frac{1}{2}(1 + ss'e^{i(\theta_{\mathbf{k}'}-\theta_{\mathbf{k}})})V(\mathbf{G})\delta_{\mathbf{k}',\mathbf{k}-\mathbf{G}} \quad (28)$$

and

$$\langle\psi^0_{s,\mathbf{k}}|-ev_0/c\sigma_y A_y(\mathbf{r})|\psi^0_{s',\mathbf{k}'}\rangle = ev_0/c\sum_{\mathbf{G}}\frac{i}{2}(s'e^{i\theta_{\mathbf{k}'}} - se^{-i\theta_{\mathbf{k}}})A_y(\mathbf{G})\delta_{\mathbf{k}',\mathbf{k}-\mathbf{G}}, \quad (29)$$

respectively. Here, **G** is a superlattice reciprocal lattice vector and $V(\mathbf{G})$ and $A_y(\mathbf{G})$ are the corresponding Fourier components of the external periodic scalar and vector potentials, respectively. Therefore, the energy dispersion and eigenstates of the quasiparticles in a graphene superlattice are obtained non-perturbatively within the single-particle picture by solving the following set of linear equations

$$(E-E^0_{s,\mathbf{k}})c(s,\mathbf{k}) = \sum_{s',\mathbf{G}} \frac{1}{2}(1+ss'e^{i(\theta_{\mathbf{k}}-\theta_{\mathbf{k}})})V(\mathbf{G})c(s',\mathbf{k}-\mathbf{G}) \tag{30}$$

for graphene under an external periodic scalar potential, and by solving the following set of linear equations

$$(E-E^0_{s,\mathbf{k}})c(s,\mathbf{k}) = \sum_{s',\mathbf{G}} \frac{1}{2}(s'e^{i\theta_{\mathbf{k}}}-se^{-i\theta_{\mathbf{k}}})A_y(\mathbf{G})c(s',\mathbf{k}-\mathbf{G}), \tag{31}$$

for graphene under an external periodic vector potential, where E is the superlattice energy eigenvalue and we have used Eqs. (3), (28), and (29). The amplitudes $c(s,\mathbf{k})$ and $c(s',\mathbf{k}-\mathbf{G})$ indicate the mixing among different unperturbed quasiparticle states of pristine graphene.

Note that the scattering amplitude methods presented here are applicable to 2D graphene superlattices in general and not just to 1D periodic systems.

5. Emerging new massless Dirac fermions in a strong external periodic scalar potential

If the external periodic scalar potential applied to graphene is sufficiently strong, new branches of massless Dirac fermions are generated near the original Dirac cone (i.e., zero-energy modes) [8–11]. Note that these new zero-energy modes are different from the new massless Dirac fermions discussed in Section 2, which have higher energies and are generated at the supercell Brillouin zone boundary centers ($\mathbf{k}=\mathbf{G}_m/2$) no matter how weak the perturbing potential is. As shown in Fig. 2, the number of zero-energy Dirac modes increases with the amplitude of the external periodic scalar potential. These new zero-energy modes could have distinguishable signatures in quantum Hall [8] or transport measurement [9].

The new zero-energy modes are generated when the applied periodic scalar potential $V(x)$ has both even and odd symmetries (Fig. 2 or 3(a) and (b)). When the odd symmetry is broken (Fig. 3(c)), new massless Dirac fermions are generated but the energy position could be different from zero (Fig. 3(d)). But, if the even symmetry is broken (Fig. 3(e)), new massless Dirac fermions are not generated (Fig. 3(f)). However, even in these broken-symmetry cases, the signatures of the modified electronic bandstructure could be captured in, e.g., Landau level measurements [8].

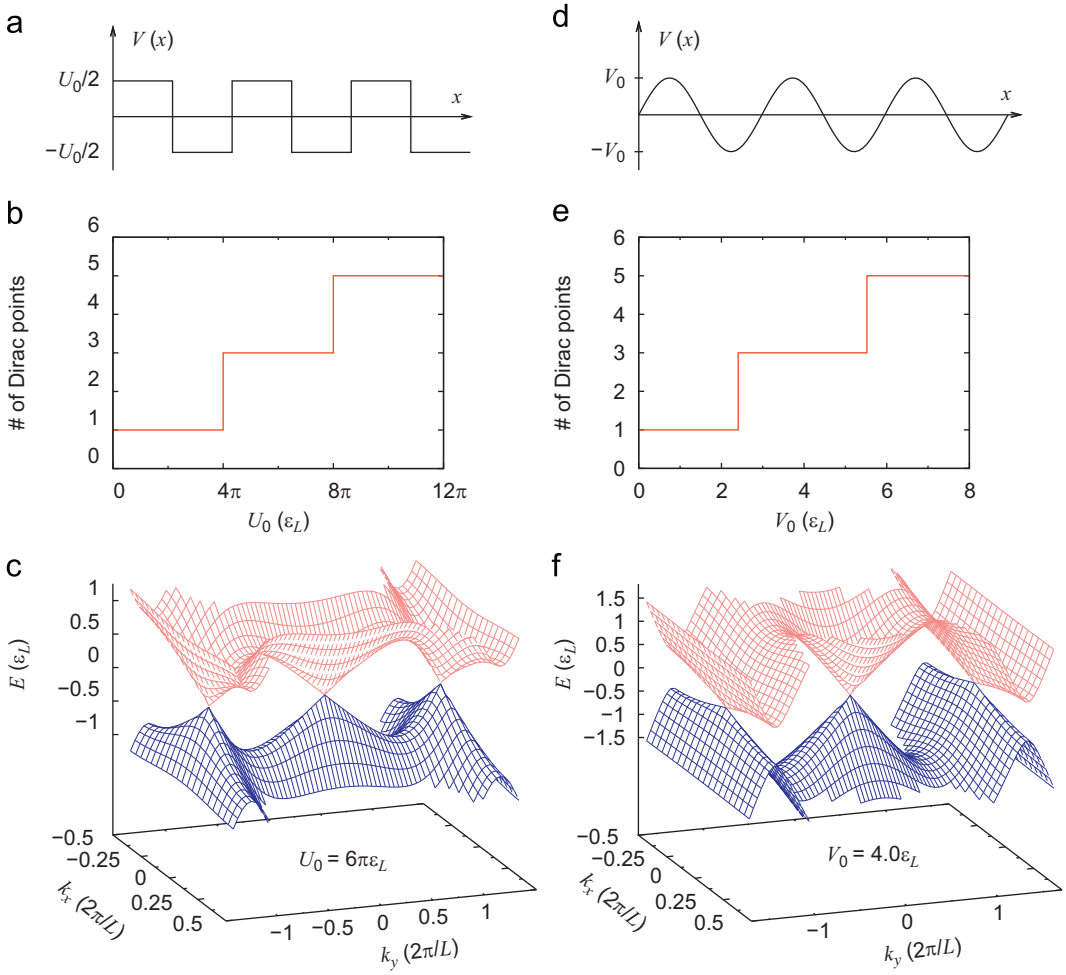

Fig. 2. (a) Schematic diagram of a Kronig–Penney type of scalar potential applied to graphene given by $U_0/2$ for $0<x<L/2$ and $-U_0/2$ for $L/2<x<L$ with lattice period L. (b) Number of Dirac points (not including spin and valley degeneracies) in a graphene superlattice versus U_0. (c) Electron energy in units of ε_L ($\equiv \hbar v_0/L$; for example, if $L=20$ nm, $\varepsilon_L=33$ meV) versus wavevector near the Dirac point for a graphene superlattice formed by the periodic scalar potential depicted in (a) with $U_0=6\pi\varepsilon_L$. (d)–(f) Same quantities as in (a)–(c) for a graphene superlattice formed by a sinusoidal scalar potential $V(x)=V_0\sin(2\pi x/L)$. In (f), $V_0=4.0\varepsilon_L$ was used.

It is worthwhile to focus on the conditions on the external periodic potential under which the number of zero-modes jumps, as shown by the steps in Fig. 2(b) and (e). We call these systems at the jump special graphene superlattices (SGSs) [5,8]. In an SGS, the group velocity along the k_y direction vanishes. Fig. 4 shows that the energy dispersion in an SGS is quasi-1D and the pseudospin in an SGS is either parallel or antiparallel to the $+k_x$ (or periodic) direction [5]. Because of this quasi-1D electron energy bandstructure in an SGS, the group velocity of electronic states are almost the same over a wide region in momentum space; and this has led to the prediction that SGSs can be used for electron beam supercollimation [5].

6. Summary

The electronic structure of graphene under a general external periodic scalar potential is modified from that of graphene in

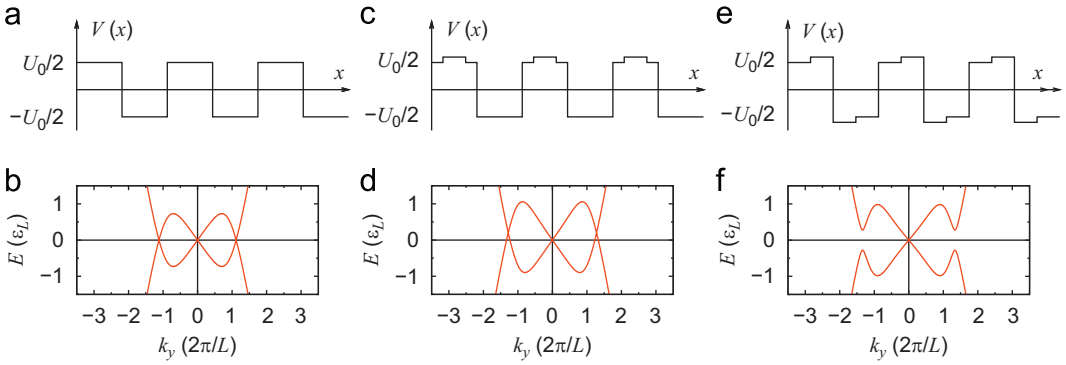

Fig. 3. (a) Kronig–Penney type of potential $V(x)$ given by $U_0/2$ for $0<x<L/2$ and $-U_0/2$ for $L/2<x<L$ with lattice period L. (b) Electron energy (in units of $\varepsilon_L=\hbar v_0/L$) versus k_y with $k_x=0$ in a graphene superlattice formed by the periodic potential in (a) with $U_0=6\pi\varepsilon_L$. (c) and (d) Same quantities as in (a) and (b) for a periodic potential $V(x)$ with a perturbation that breaks the odd symmetry. The perturbing potential $\Delta V(x)$ within one unit cell is given by +10% of the potential amplitude $(U_0/2)$ for $L/8<x<3L/8$ and zero otherwise. (e) and (f) Same quantities as in (a) and (b) for a periodic potential $V(x)$ with a perturbation that breaks the even symmetry. The perturbing potential $\Delta V(x)$ within one unit cell is given by +10% and −10% of the potential amplitude $(U_0/2)$ for $L/4<x<L/2$ and for $L/2<x<3L/4$, respectively, and zero otherwise.

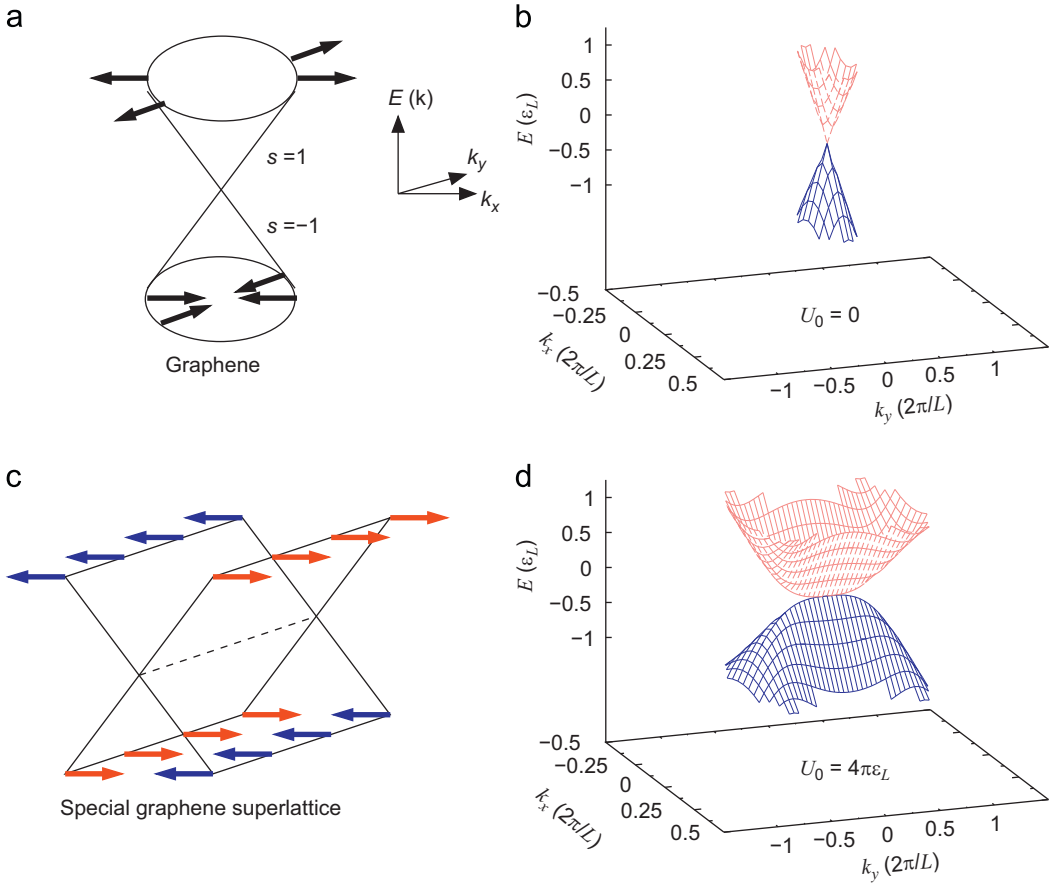

Fig. 4. (a) Schematic diagram showing the electronic energy dispersion relations and pseudospin vectors (black arrows) in graphene. (b) Calculated electron energy bandstructure in graphene. (c) and (d): Same quantity as in (a) and (b), respectively, for the considered Kronig–Penney type of an SGS (as defined in Fig. 1(b) with $U_0=4\pi\varepsilon_L$ where $\varepsilon_L=\hbar v_0/L$). Red and blue arrows in (c) represent the 'right' and the 'left' pseudospin state, respectively. (For interpretation of the references to colour in this figure legend, the reader is referred to the web version of this article.)

several highly unexpected ways: (i) the group velocity is anisotropically renormalized in momentum space and (ii) new massless Dirac fermions are generated at the supercell Brillouin zone boundary. Moreover, when a strong 1D periodic scalar potential is applied, new zero-energy modes emerge. Under certain conditions, the group velocity of charge carriers along the direction perpendicular to the 1D periodic direction of the superlattice potential vanishes. In this special class of 1D graphene superlattices, the electron energy bandstructure and pseudospin structure are quasi-1D and these properties can be used in collimating the electron flow. With a 1D external periodic vector potential applied to graphene, on the other hand, the group velocity of charge carriers near the original Dirac point is reduced isotropically. The analytical and numerical methods discussed in this paper can be used in further investigating the novel properties of quasiparticles in 1D and 2D graphene superlattices.

Acknowledgments

We acknowledge Li Yang, Young-Woo Son, and Marvin L. Cohen for fruitful discussions and collaboration. The theoretical part of this work was supported by NSF Grant no. DMR07-05941, and L.Z.T. and the simulation part of the study by the Director, Office of Science, Office of Basic Energy Sciences, Division of Materials Sciences and Engineering Division, U.S. Department of Energy under Contract no. DE-AC02-05CH11231. C.-H.P. was supported by Office of Naval Research MURI Grant no. N00014-09-1066. Computational resources have been provided by TeraGrid and NERSC.

References

[1] A.H. Castro Neto, F. Guinea, N.M.R. Peres, K.S. Novoselov, A.K. Geim, Rev. Mod. Phys. 81 (2009) 109.
[2] C. Bai, X. Zhang, Phys. Rev. B 76 (2007) 075430.
[3] C.-H. Park, L. Yang, Y.-W. Son, M. Cohen, S.G. Louie, Nature Phys. 4 (2008) 213.
[4] M. Barbier, F.M. Peeters, P. Vasilopoulos, J.J. Milton Pereira, Phys. Rev. B 77 (11) (2008) 115446.
[5] C.-H. Park, Y.-W. Son, L. Yang, M.L. Cohen, S.G. Louie, Nano Lett. 8 (2008) 2920.
[6] C.-H. Park, L. Yang, Y.-W. Son, M.L. Cohen, S.G. Louie, Phys. Rev. Lett. 101 (2008) 126804.
[7] J.H. Ho, Y.H. Chiu, S.J. Tsai, M.F. Lin, Phys. Rev. B 79 (2009) 115427.
[8] C.-H. Park, Y.-W. Son, L. Yang, M.L. Cohen, S.G. Louie, Phys. Rev. Lett. 103 (2009) 046808.
[9] L. Brey, H.A. Fertig, Phys. Rev. Lett. 103 (2009) 046809.
[10] M. Barbier, P. Vasilopoulos, F.M. Peeters, Phys. Rev. B 81 (2010) 075438.
[11] L.-G. Wang, S.-Y. Zhu, Phys. Rev. B 81 (2010) 205444.
[12] M.R. Masir, P. Vasilopoulos, A. Matulis, F.M. Peeters, Phys. Rev. B 77 (2008) 235443.
[13] M.R. Masir, P. Vasilopoulos, F.M. Peeters, Phys. Rev. B 79 (2009) 035409.
[14] S. Ghosh, M. Sharma, J. Phys. Cond. Matt. 21 (2009) 292204.
[15] L. Dell'Anna, A.D. Martino, Phys. Rev. B 79 (2009) 045420.
[16] Q.-S. Wu, S.-N. Zhang, S.-J. Yang, J. Phys. Cond. Matt. 20 (2008) 485210.
[17] I. Snyman, Phys. Rev. B 80 (2009) 054303.
[18] L.Z. Tan, C.-H. Park, S.G. Louie, Phys. Rev. B 81 (2010) 195426.
[19] A. Isacsson, L.M. Jonsson, J.M. Kinaret, M. Jonson, Phys. Rev. B 77 (2008) 035423.
[20] F. Guinea, M.I. Katsnelson, M.A.H. Vozmediano, Phys. Rev. B 77 (2008) 075422.
[21] T.O. Wehling, A.V. Balatsky, M.I. Katsnelson, A.I. Lichtenstein, Europhys. Lett. 84 (2008) 17003.
[22] J.C. Meyer, C.O. Girit, M.F. Crommie, A. Zettl, Appl. Phys. Lett. 92 (2008) 123110.
[23] S. Marchini, S. Günther, J. Wintterlin, Phys. Rev. B 76 (2007) 075429.
[24] A.L. Vazquez de Parga, F. Calleja, B. Borca, M.C.G. Passeggi Jr., J.J. Hinarejo, F. Guinea, R. Miranda, Phys. Rev. Lett. 100 (2008) 056807.
[25] P.W. Sutter, J.-I. Flege, E.A. Sutter, Nature Mater. 7 (2008) 406.
[26] D. Martoccia, P.R. Willmott, T. Brugger, M. Björck, S. Günther, C.M. Schlepütz, A. Cervellino, S.A. Pauli, B.D. Patterson, S. Marchini, J. Wintterlin, W. Moritz, T. Greber, Phys. Rev. Lett. 101 (2008) 126102.
[27] J. Coraux, A.T. N'Diaye, C. Busse, T. Michely, Nano Lett. 8 (2008) 565.
[28] A.T. N'Diaye, J. Coraux, T.N. Plasa, C. Busse, T. Michely, New J. Phys. 10 (2008) 043033.
[29] I. Pletikosić, M. Kralj, P. Pervan, R. Brako, J. Coraux, A.T. N'Diaye, C. Busse, T. Michely, Phys. Rev. Lett. 102 (2009) 056808.
[30] W. Bao, F. Miao, Z. Chen, H. Zhang, W. Jang, C. Dames, C.N. Lau, Nature Nanotechnol. 4 (2009) 562.
[31] T. Ando, T. Nakanishi, J. Phys. Soc. Jpn. 67 (1998) 1704.
[32] P.L. McEuen, M. Bockrath, D.H. Cobden, Y.-G. Yoon, S.G. Louie, Phys. Rev. Lett. 83 (1999) 5098.
[33] P.R. Wallace, Phys. Rev. 71 (1947) 622.
[34] V.I. Talyanskii, D.S. Novikov, B.D. Simons, L.S. Levitov, Phys. Rev. Lett. 87 (2001) 276802.
[35] D.S. Novikov, Phys. Rev. B 72 (2005) 235428.
[36] H. Ajiki, T. Ando, J. Phys. Soc. Jpn. 62 (1993) 1255.
[37] H.-W. Lee, D.S. Novikov, Phys. Rev. B 68 (2003) 155402.